

Statistics of the hot spots of smoothed beams produced by random phase plates revisited

J. Garnier^{a)}

*Centre de Mathématiques Appliquées, Centre National de la Recherche Scientifique,
Unité Mixte de Recherche 7641, Ecole Polytechnique, 91128 Palaiseau Cedex, France*

(Received 21 August 1998; accepted 28 January 1999)

This paper revisits and corrects the statistical theory of hot spots of speckle patterns such as those produced by a random phase plate. Analytical expressions are derived which are sensitively different from the previous results of Rose and DuBois [Phys. Fluids B **5**, 590 (1993)]. The departure essentially originates from a careful approach which takes into account the fact that the fields are complex-valued, while the standard mathematical theory deals with the maxima of real-valued Gaussian fields. This gives rise to an enhancement of the number of the most intense hot spots. Excellent agreements between the theoretical formulas and numerical simulations are shown.

© 1999 American Institute of Physics. [S1070-664X(99)02205-3]

I. INTRODUCTION

Smoothing techniques are extensively studied for inertial confinement fusion (ICF) applications. The future French Laser MegaJoule (LMJ) and the US National Ignition Facility (NIF)¹ are designed for the indirect drive scheme, whose principle is the following. Numerous laser beams are focused into a hohlraum and irradiate the inner gold wall to produce x-rays. However, it was found that it is necessary to diminish the wall expansion by filling the cavity by a gas. Unfortunately, this means that the laser light has to propagate through an underdense plasma where parametric instabilities such as stimulated Raman scattering (SRS) or stimulated Brillouin scattering (SBS) may occur. Since experimental evidence of SRS and SBS in hohlraums from randomized laser beams has been observed,²⁻⁶ the control of high laser intensities has become of crucial importance.

The literature contains a lot of work which deals with self-focusing (SF) and/or parametric instabilities from optically smoothed beams. Most of the theoretical papers develop careful methods to study SBS and/or SF⁷⁻⁹ from a single speckle and then average the single hot spot reflectivity over the statistics of hot spots. It is thus of great interest to have precise expressions for the probability density of the intensities of the hot spots of a speckle pattern.

The statistical distribution of the maximal intensities of the hot spots can be calculated theoretically for a focal spot in vacuum or homogeneous medium, in the asymptotic framework where the number of spatial modes is large, so that the Gaussian limit is valid.^{10,11} The corresponding distribution is then entirely characterized by the autocorrelation function of the field, which can also be computed very precisely for any smoothing method.¹² The theory developed in Ref. 10 is based on the ansatz that the number of intense hot spots above a given intensity is proportional to the number of local maxima of the real part of the field. Unfortunately the formulas derived by this method have some free parameters

that have to be determined through numerical simulations (Ref. 11). Furthermore, we feel that the hot spot ansatz should be carefully checked. In this paper we shall revisit the ansatz and obtain closed form expressions for the number of intense hot spots which do not coincide exactly with the previous formulas.

This work is triggered by the study of the statistics of local maxima of the speckle patterns generated by random phase plates (RPP)¹³ or kinoform phase plates (KPP).¹⁴ Although very careful attention is devoted to this case, the formulas we derive in our paper can be applied to more general situations where the Gaussian limit is valid. We focus our attention on structures which are small compared to the finite extent of the laser beam. For the sake of simplicity and without loss of generality, we shall consider translationally invariant beams.

We begin with a brief review of what is known in the mathematical literature about the local maxima of *real*-valued random fields with Gaussian statistics. We study the local maxima of *complex*-valued fields with Gaussian statistics under the hypothesis that the real and imaginary parts of the field are statistically independent, which is equivalent to assume that the correlation function of the field is real valued. We derive very general formulas which can then be applied to the hot spots of a speckle pattern generated by a RPP in the focal plane. Unfortunately, in the focal volume, the hypothesis of the independence of the real and imaginary parts of the field does not hold true, but we are able to perform a specific analysis which gives complete expressions for the statistics of the hot spots of the speckle pattern generated by a RPP in the focal volume.

II. MAXIMA OF REAL GAUSSIAN FIELDS

We begin with a key theoretical result concerning local maxima of real-valued Gaussian fields, which we then apply to complex-valued Gaussian fields in the next sections. Let X be a statistically homogeneous, real-valued, zero mean Gaussian family with variance σ^2 defined over the real space

^{a)}Electronic mail: garnier@cmapx.polytechnique.fr

\mathbb{R}^d of dimension d (or a subset of \mathbb{R}^d) and let M_u^X be the number of local maxima of X^2 which are above the level u in some volume V . Then, by denoting

$$\Psi_j(u) = \frac{(-1)^j C_d^{2j} (2j)! \sigma^{2j}}{j! 2^{(d+2j+1)/2} \pi^{(d+1)/2}} \int_{\sqrt{u}}^{\infty} x^{d-2j} \exp\left(-\frac{x^2}{2\sigma^2}\right) dx,$$

one can refine results of Adler (Ref. 15, Theorem 6-3-1) and establish that¹⁶

$$\langle M_u^X \rangle = \frac{2|V| |\det \Lambda|^{1/2}}{\sigma^{2d+1}} \sum_{j=0}^{\lfloor d/2 \rfloor} \Psi_j(u) + \mathcal{O}\left(\frac{\exp(-u/2\sigma^2)}{(u/\sigma^2)^{\alpha/2}}\right), \quad (1)$$

where α is any positive number and Λ is the matrix of the second-order spectral moments of the process X :

$$\Lambda_{ij} = \left\langle \frac{\partial X}{\partial x_i}(0) \frac{\partial X}{\partial x_j}(0) \right\rangle. \quad (2)$$

III. STATISTICS OF THE HOT SPOTS OF A SPECKLE PATTERN

Let us consider a complex-valued Gaussian field A , that is to say, a field which is the superposition of two independent real-valued Gaussian fields A_R and A_I with the same statistics and variances $I_0/2$,

$$A = A_R + iA_I.$$

The autocorrelation function of the field A is denoted by

$$C(\mathbf{x}) = \langle A(\mathbf{y} + \mathbf{x}) A^*(\mathbf{y}) \rangle.$$

The matrix Λ which appears in the above section corresponds to $X = A_R$ or A_I and is given by

$$\Lambda_{ij} = \frac{1}{2} \left\langle \frac{\partial A}{\partial x_i} \frac{\partial A^*}{\partial x_j} \right\rangle = -\frac{1}{2} \left. \frac{\partial^2 C}{\partial x_i \partial x_j} \right|_{\mathbf{x}=0}.$$

Given some domain V , the number of maxima of A_R^2 (resp. A_I^2) above the level u is denoted by $M_u^{A_R}$ (resp. $M_u^{A_I}$). In this section we deal with the statistics of the number M_u^A of local maxima (the so-called hot spots) of the intensity distribution $|A|^2$ above the level u .

In Ref. 10 Rose and DuBois assume the following ansatz: “the relative frequency of intense hot spots with a given intensity is the same as the relative frequency of intense local maxima of A_R^2 ,” which implies that the number M_u^A of hot spots above the level u is proportional to the sum of the numbers of maxima of A_R^2 and A_I^2 . This also reads as

$$\langle M_u^A \rangle_{R\&D} \sim \frac{|V| |\det \Lambda|^{1/2} 2^{(d+2)/2}}{\pi^{(d+1)/2} I_0^{d/2}} \left(\frac{u}{I_0}\right)^{(d-1)/2} \exp\left(-\frac{u}{I_0}\right).$$

We shall follow the same strategy but we revisit the ansatz of Rose and DuBois. It is based upon the fact that A_R and A_I are independent in any point \mathbf{x}_0 . Because of this independence, if the point \mathbf{x}_0 is a local maximum of A_R^2 , then \mathbf{x}_0 has no particular property in the point of view of A_I^2 . By definition of a Gaussian process, $A_I(\mathbf{x}_0)$ then obeys a real-valued Gaussian random variable, with variance $I_0/2$. In Refs. 10 and 11 Rose and DuBois then considered the contribution of A_I^2 as a negligible perturbation. But we shall see

that this is rigorously not correct. We claim that “the intense local maxima of the intensity distribution correspond to local maxima of A_R^2 (or A_I^2), the contribution of A_I^2 (or A_R^2) being smaller, following the square of a Gaussian random variable with variance $I_0/2$.” This statement actually proposes an ansatz to deduce the statistical distribution of the maximal value of the intensity $A_R^2 + A_I^2$ from the one of the real part A_R . Our own ansatz is carefully checked in Appendix B. Let us apply it and compute the mean number $\langle M_u^A \rangle$ of local maxima of the intensity distribution above the level u . Such a maximum is produced either by a local maximum of A_R^2 or A_I^2 . Thus the number of maxima of $|A|^2$ above u inside the domain V is

$$M_u^A = \sum_{x \in U(A_R)} \mathbb{1}_{A_R^2(x) + a_I^2(x) \geq u} + \sum_{x \in U(A_I)} \mathbb{1}_{A_I^2(x) + a_R^2(x) \geq u},$$

where $\mathbb{1}_{\{\dots\}}$ is equal to 1 if the condition $\{\dots\}$ is true and 0 otherwise, and $U(A_R)$ (resp. $U(A_I)$) is the set of the loci of the maxima of A_R^2 (resp. A_I^2) inside V . The $a_I(\cdot)$ and $a_R(\cdot)$ are independent Gaussian random variables with zero means and variances $I_0/2$. So the a_I^2 's and a_R^2 's obey the same distribution whose common density with respect to the Lebesgue measure over \mathbb{R}^+ is $p(v) = 1/(\sqrt{\pi} I_0)(v/I_0)^{-1/2} \times \exp(-v/I_0)$. Taking the expectation we get that the mean number of local maxima above the level u of the intensity $|A|^2$ is given by the convolution:

$$\langle M_u^A \rangle = \int_0^{v_m} \langle M_{u-v}^{A_R} \rangle p(v) dv + \int_0^{v_m} \langle M_{u-v}^{A_I} \rangle p(v) dv.$$

It remains to determine v_m . The natural choice for such a convolution would be $v_m = u$. Nevertheless, we claim that the correct choice for v_m is $v_m := u/2$. Indeed, consider in the first integral the contribution of the convoluted integrand for some $v > u/2$. Then note that $v > u/2$ means that $a_I^2 > A_R^2$ so that the maximum of $|A|^2$ is also very close to some maximum above the level $u/2$ of the imaginary part A_I^2 of the field. But this maximum is already taken into account in the second integral. One must consequently stop the integration with respect to the density $p(v)$ at level $u/2$, since otherwise one would count some maxima twice. $v_m := u/2$ is the only choice which leads to count each maximum of A_R^2 and A_I^2 once and only once. Symmetry arguments further show that $\langle M_u^{A_R} \rangle = \langle M_u^{A_I} \rangle$, so that we get

$$\langle M_u^A \rangle = 2 \int_0^{u/2} \langle M_{u-v}^{A_R} \rangle p(v) dv. \quad (3)$$

Combining with Eq. (1) with $\sigma^2 = I_0/2$,

$$\begin{aligned} \langle M_u^A \rangle &= \frac{|V| |\det \Lambda|^{1/2} 2^{(d+2)/2}}{I_0^{(d+2)/2} \pi^{(d+2)/2}} \\ &\times \left(C_d \left(\frac{u}{I_0}\right)^{d/2} + C_d' \left(\frac{u}{I_0}\right)^{(d-2)/2} \right) \exp\left(-\frac{u}{I_0}\right), \quad (4) \end{aligned}$$

where

$$C_d = \int_0^{1/2} \frac{(1-v)^{(d-1)/2}}{\sqrt{v}} dv = 2 \int_0^{\pi/4} (\cos \theta)^d d\theta,$$

$$C'_d = \frac{d}{2} C_d - \frac{d(d-1)}{4} C_{d-2}.$$

In particular $C_2 = 1/2 + \pi/4$, $C'_2 = 1/2$, $C_3 = 5\sqrt{2}/6$ and $C'_3 = -\sqrt{2}/4$, so that we get the explicit formulas:

(1) If $d=2$ (two-dimensional case), then

$$\langle M_u^A \rangle = \frac{4|S||\det\Lambda|^{1/2}}{\pi^2 I_0} \left(\left(\frac{1}{2} + \frac{\pi}{4} \right) \frac{u}{I_0} + \frac{1}{2} \right) \exp - \frac{u}{I_0}, \quad (5)$$

where S is the reference surface.

(2) If $d=3$ (three-dimensional case), then

$$\langle M_u^A \rangle = \frac{20|V||\det\Lambda|^{1/2}}{3\pi^{5/2}I_0^{3/2}} \left(\left(\frac{u}{I_0} \right)^{3/2} - \frac{3}{10} \left(\frac{u}{I_0} \right)^{1/2} \right) \exp - \frac{u}{I_0}, \quad (6)$$

where V is the reference volume.

IV. NUMERICAL SIMULATIONS

In order to test the formulas (5) and (6) we have carried out numerical simulations in the two- and three-dimensional cases (2D and 3D). The routine to simulate a stationary Gaussian field with any correlation function C is described in the following section..

A. Simulation of a Gaussian field

We describe here the routine to simulate a two-dimensional stationary Gaussian field. The generalization to any dimension is straightforward, at the expense of having to add more and more indices. First note that the Fourier transform of C is non-negative real-valued. Indeed the Fourier transform of the correlation function of a stationary Gaussian field is proportional to its power spectral density which is obviously non-negative.¹⁷ The physical computation domain is a square of size $[0, Nh] \times [0, Nh]$ with elementary step h . Consider a $N \times N$ array $X_{j,l}$ of independent, complex-valued, zero-mean and Gaussian random variables with $\langle |X_{j,l}|^2 \rangle = 1$. This array is a discrete Gaussian white noise. Then one has to filter it in three steps. First apply the discrete Fourier transform on the array:

$$\hat{X}_{u,v} = \sum_{j,l=0}^{N-1} X_{j,l} \exp i(2\pi(ju + lv)/N).$$

Then multiply it by $\sqrt{\hat{C}}$, where \hat{C} is the discrete Fourier transform of the correlation function C :

$$\hat{C}_{u,v} = \sum_{j,l=0}^{N-1} C(jh, lh) \exp i(2\pi(ju + lv)/N),$$

$$\tilde{X}_{u,v} = \hat{X}_{u,v} \sqrt{\hat{C}_{u,v}}.$$

Finally apply the discrete inverse Fourier transform:

$$\bar{X}_{j,l} = \frac{1}{N^2} \sum_{u,v=0}^{N-1} \tilde{X}_{u,v} \exp -i(2\pi(ju + lv)/N).$$

The resulting $N \times N$ array \bar{X} is precisely a realization of a Gaussian field with correlation function C :

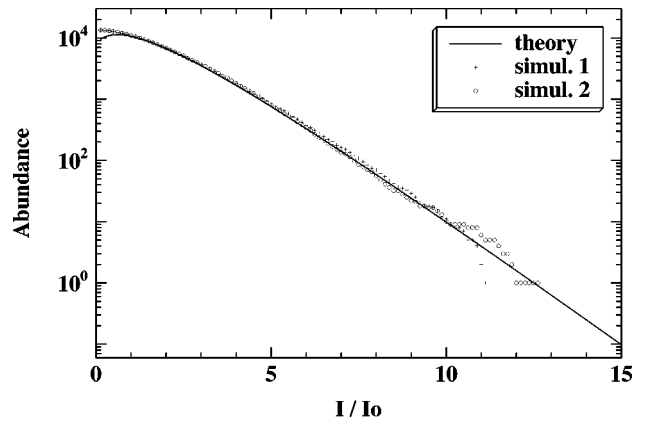


FIG. 1. Abundance M_l^A of local maxima of the intensity above level I . Here $d=2$, $C(x,y) = \exp(-(x^2+y^2)/\rho_c^2)$ ($|\det\Lambda| = \rho_c^{-4}$) with $\rho_c = 0.005$ and $|S| = 1$. Results corresponding to two different simulations (crosses and circles) and the theoretical mean abundance (solid line) corresponding to Eq. (5) are shown.

$$\bar{X}_{j,l} = A(jh, lh), \quad j, l \in \{0, \dots, N-1\}.$$

The three steps of the filter are in fact linear operations, which consequently conserve the Gaussian property of the initial field X . Furthermore, it is obvious to establish that \bar{X} possesses the desired correlation function. If we denote by \bar{C} the inverse Fourier transform of $\sqrt{\hat{C}}$, then \bar{X} is simply the convoluted array $X \star \bar{C}$:

$$\bar{X}_{j,l} = \frac{1}{N^2} \sum_{j',l'=0}^{N-1} X_{[j-j']N+l',l'} \bar{C}_{j',l'}.$$

If j is an integer ($j \in \mathbb{N}$), then there exists a unique couple of integers $(j_1, j_2) \in \mathbb{N} \times [0, N]$ such that $j = j_1 N + j_2$, and we denote j_2 by $[j]$. Since the $X_{j,l}$ are independent from each other and zero mean, straightforward calculations yield

$$\langle \bar{X}_{j_1, l_1} \bar{X}_{j_2, l_2}^* \rangle = (\bar{C} \star \bar{C}^*)_{[j_1-j_2]N, [l_1-l_2]}.$$

In this expression the exponent $*$ holds for complex conjugation while the sign \star holds for the discrete convolution. The convoluted array $\bar{C} \star \bar{C}^*$ is the inverse Fourier transform of the multiplied array $\sqrt{\hat{C}} \cdot \sqrt{\hat{C}^*} = |\hat{C}|$. Since \hat{C} is non-negative real valued, we have $|\hat{C}| = \hat{C}$ so that the array $\bar{C} \star \bar{C}^*$ is exactly C .

B. Analysis

Figures 1 and 2 compare the theoretically and numerically determined numbers of local maxima above some level I of two- and three-dimensional speckle patterns with Gaussian statistics and Gaussian correlation function. They show excellent agreement between the theoretical formulas (5) and (6) and the corresponding simulations.

V. SPECKLE PATTERN WITH A SLOWLY VARYING ENVELOPE

In the above sections we have considered a standard speckle pattern whose mean intensity is constant over the

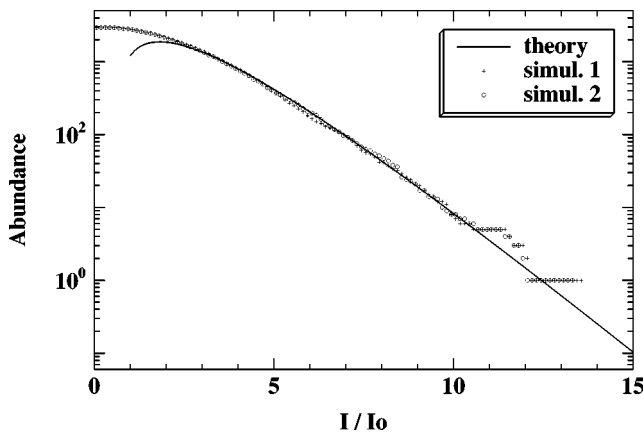


FIG. 2. Abundance M_l^A of local maxima of the intensity above level I . Here $d=3$, $C(x,y,z)=\exp(-(x^2+y^2+z^2)/\rho_c^2)$ ($|\det|\Lambda|=\rho_c^{-6}$) with $\rho_c=0.04$ and $|V|=1$. Results corresponding to two different simulations (crosses and circles) and the theoretical mean abundance (solid line) corresponding to Eq. (6) are shown.

reference domain V . We now regard a speckle pattern whose intensity distribution has an overall slowly varying envelope $E(\mathbf{x})$ so that the field can be represented as $A(\mathbf{x})E(\mathbf{x})^{1/2}$ where A is a complex-valued field with Gaussian statistics and constant mean intensity as described in Sec. III. For any domain V , we denote by $M_u^{AE^{1/2},V}$ (resp. $M_u^{A,V}$) the number of maxima above level u of the speckle pattern $A(\mathbf{x})E(\mathbf{x})^{1/2}$ [resp. $A(\mathbf{x})$] over the domain V . We aim at computing $\langle M_u^{AE^{1/2},V_{tot}} \rangle$ where V_{tot} stands for the whole space \mathbb{R}^d . Choosing $I \ll \sup_{\mathbf{x} \in V_{tot}} E(\mathbf{x})$, we consider the partition $(V_n)_{n \in \mathbb{N}}$ of the whole domain V_{tot} given by

$$V_n := \{\mathbf{x} \in V_{tot} \text{ s. t. } E(\mathbf{x}) \in [nI, (n+1)I)\}.$$

The results of Sec. III can be applied to the domains V_n where the mean intensity [governed by the variations of $E(\mathbf{x})$] is almost constant. Furthermore, formula (4) implies that, for any $\alpha > 0$, the mean number of maxima above level u of a standard speckle pattern with mean intensity αI_0 is equal to the mean number of maxima above level u/α of a standard speckle pattern with mean intensity I_0 . Consequently,

$$\langle M_u^{AE^{1/2},V_n} \rangle = \langle M_{u/(nI)}^{A,V_n} \rangle$$

and, summing over n ,

$$\langle M_u^{AE^{1/2},V_{tot}} \rangle = \sum_n \langle M_{u/(nI)}^{A,V_n} \rangle.$$

Since $\langle M_{u/(nI)}^{A,V_n} \rangle$ is proportional to the volume $|V_n|$, the sum can be rewritten as

$$\langle M_u^{AE^{1/2},V_{tot}} \rangle = \int \langle M_{u/E(\mathbf{x})}^{A,1} \rangle d\mathbf{x}, \tag{7}$$

where $\langle M_{u/E(\mathbf{x})}^{A,1} \rangle$ is the mean number of maxima above level u of the speckle pattern $A(\mathbf{x})$ over a domain with volume one.

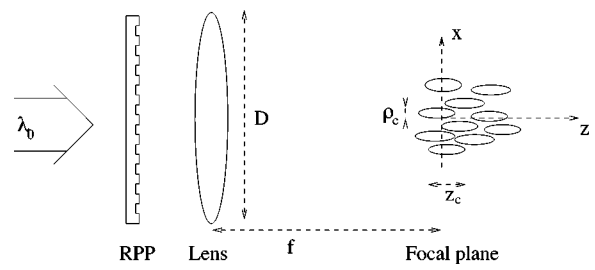


FIG. 3. The RPP configuration.

VI. APPLICATION TO THE SPECKLE PATTERN GENERATED BY A RPP

A. Formulation

The standard model of RPP can be ideally characterized as follows (see Fig. 3). A monochromatic pulse illuminates a square RPP, which consists of square elements imposing randomly a phase shift of 0 or π . Each element of the RPP generates a beamlet which is focused in the focal plane of the lens. The far-field intensity distribution then consists of an overall envelope function determined by the RPP element superimposed with a fine speckle pattern arising due to the interference among the various RPP elements. The binary RPPs are currently used¹³ and they produce a far-field intensity envelope which is essentially an Airy function:

$$E(x,y) = I_0 \operatorname{sinc}\left(\frac{x}{a}\right)^2 \operatorname{sinc}\left(\frac{y}{a}\right)^2, \tag{8}$$

where $\operatorname{sinc}(s) := \sin(\pi s)/(\pi s)$, $a = \lambda_0 f/h$ is the width of the focal spot, λ_0 is the carrier wavelength of the incident wave, h is the length of the side of a square element of the RPP, and f is the lens focal length. This specific choice for the envelope function does not appreciably affect the underlying speckle statistics. In Ref. 18 the authors carefully consider a realistic experimental configuration and analyze the statistics of the speckle intensity $I(x,y)$ after the far-field intensity pattern is divided by the envelope function $E(x,y)$. They show that the histogram of $I(x,y)/E(x,y)$ follows closely the exponential distribution characteristic of a standard speckle pattern. A similar conclusion follows from Ref. 19: If one removes the envelope function from the far-field intensity distribution, then it is observed that the remaining speckle pattern is a standard speckle pattern whenever the number of contributing phase plates elements is sufficiently large. Consequently, one can study the number of local maxima above level u in some small surface or volume where the mean intensity is locally constant. Formula (7) will then give the number of local maxima above level u in the whole focal spot. We consider points in the focal plane such that $x,y \ll a$, so that the smooth sinc envelope of the diffraction function of a square aperture can be considered as quasi-uniform. In this region of the focal spot, the beamlets generated by the elements of the RPP interfere and form a speckle pattern:

$$A(x,y) = \frac{\sqrt{I_0}}{2N+1} \sum_{j,l=-N}^N \exp i \left(\pi \frac{jx+ly}{N\rho_c} + \phi_{j,l} \right), \tag{9}$$

where ρ_c is the correlation radius,

$$\rho_c := \frac{\lambda_0 f}{D}, \tag{10}$$

D is the near-field square beam aperture, and $(2N+1)^2$ is the number of elements of the square RPP, i.e., $2N+1 = D/h$. $\phi_{j,l}$ is the random phase imposed by the j,l -th element. We assume that the $\phi_{j,l}$ are independent random variables which take either the value 0 or π with probability 1/2. The modes are normalized by the factor $\sqrt{I_0}/(2N+1)$ so that the mean intensity of the field A is I_0 . In Fourier space, the energy spectrum of A is a top hat that cuts off for $|k_x|$ or $|k_y|$ larger than $k_{\max} := \pi/\rho_c$ and which is uniform inside the square $[-k_{\max}, k_{\max}] \times [-k_{\max}, k_{\max}]$. Throughout this section we shall consider the asymptotic framework $N \gg 1$ so that the field A is a stationary, zero-mean, random process with Gaussian statistics by application of the central limit theorem.²⁰

In the paraxial approximation, and assuming that the medium is homogeneous (absence of plasma density fluctuations), the field satisfies the propagation equation:

$$2ik_0 \frac{\partial A}{\partial z} + \Delta_{\perp} A = 0,$$

where k_0 is the homogeneous wave number and Δ_{\perp} the orthogonal Laplacian. This equation implies that the field in some plane z is the superposition of the modes (j,l) changed by a phase factor $\exp -i(\pi^2/4)((j^2+l^2)/N^2)(z/z_c)$, where z_c is the longitudinal correlation length:

$$z_c := \frac{k_0 \rho_c^2}{2}. \tag{11}$$

The correlation lengths ρ_c and z_c can be rewritten in terms of the laser wavelength and the so-called F-number ($F=f/D$) as $\rho_c = \lambda_0 F$ and $z_c = \pi \lambda_0 F^2$. Furthermore, the cutoff frequency in the RPP energy spectrum then writes as $k_{\max} = k_0/(2F)$.

B. The focal plane

In the central region of the focal plane the field is the superposition of many beamlets (9). By the central limit theorem, in the asymptotic framework $N \gg 1$ the complex-valued field A obeys Gaussian statistics with mean 0 and correlation function

$$C(x,y) = I_0 \operatorname{sinc}\left(\frac{x}{\rho_c}\right) \operatorname{sinc}\left(\frac{y}{\rho_c}\right),$$

where $\operatorname{sinc}(s) := \sin(\pi s)/(\pi s)$. The corresponding matrix of the second-order spectral moments is equal to

$$\Lambda = \frac{I_0}{2} \begin{pmatrix} \lambda_x & 0 \\ 0 & \lambda_y \end{pmatrix}, \tag{12}$$

$$\lambda_{\xi} := -\frac{\partial^2 C}{\partial \xi^2}(0,0)/I_0. \tag{13}$$

Here we have $\lambda_x = \lambda_y = \pi^2/(3\rho_c^2)$ so that $|\det \Lambda|^{1/2} = I_0 \pi^2/(6\rho_c^2)$, and Eq. (5) then implies

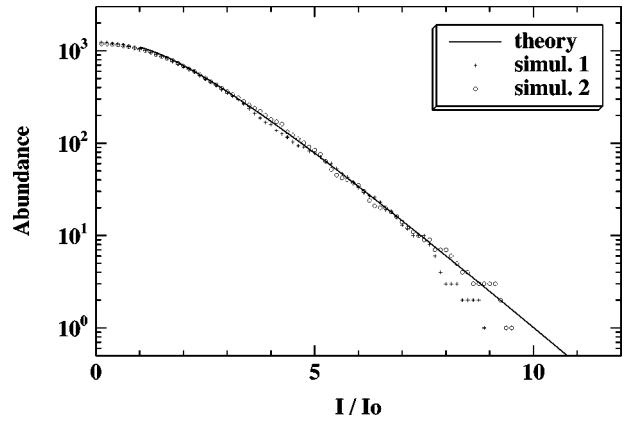


FIG. 4. Abundance M_u^{xy} of local maxima of the intensity above level I in a sub-domain S of the focal plane of a RPP. Here $N=35$, $\rho_c=0.02$ and $|S|=1$. Results corresponding to two different simulations (crosses and circles) and the mean theoretical abundance (solid line) corresponding to Eq. (14) are shown.

$$\langle M_u^{xy} \rangle = \frac{2|S|}{3\rho_c^2} \left(\left(\frac{1}{2} + \frac{\pi}{4} \right) \frac{u}{I_0} + \frac{1}{2} \right) \exp -\frac{u}{I_0}, \tag{14}$$

where S is the reference surface (see Fig. 4). This result holds true for a surface S which is small compared to the focal spot, so that we can neglect the variations of the envelope of the spot. If we take into account the overall envelope (8) and look for the expected number of local maxima above level u in the whole focal spot, then applying formula (7) and computing only the leading order term one finds that

$$\langle M_u^{\text{focal}} \rangle = \frac{2a^2}{\pi\rho_c^2} \left(\frac{1}{2} + \frac{\pi}{4} \right) \exp -\frac{u}{I_0}.$$

More generally, let us assume that the focal spot envelope has the following form:

$$E(x,y) = I_0 \exp -\frac{(x^2+y^2)^n}{r_0^{2n}}.$$

For $n=1$ we have a Gaussian envelope, while $n>1$ corresponds to a flat-top super-Gaussian envelope ($2n$ th power). Applying formula (7), we get that the expected number of local maxima of the focal spot above level u is given by the integral:

$$\begin{aligned} \langle M_u^{\text{focal}} \rangle &= \frac{2\pi r_0^2}{3\rho_c^2} \int_{R=1}^{\infty} \left(\left(\frac{1}{2} + \frac{\pi}{4} \right) \frac{u}{I_0} + \frac{1}{2R} \right) \\ &\quad \times \exp\left(-\frac{uR}{I_0}\right) \frac{(\ln R)^{1/n-1}}{n} dR. \end{aligned}$$

If we restrict ourselves to the computation of the leading order term, we then find that

$$\langle M_u^{\text{focal}} \rangle = \frac{2\pi r_0^2}{3\rho_c^2} \frac{1}{n} \Gamma\left(\frac{1}{n}\right) \left(\frac{1}{2} + \frac{\pi}{4} \right) \left(\frac{u}{I_0} \right)^{1-1/n} \exp -\frac{u}{I_0},$$

where $\Gamma(s) := \int_0^{\infty} r^{s-1} e^{-r} dr$ is the so-called Euler's gamma function. In case of an almost perfect flat-top envelope $n \rightarrow \infty$, we get back the formula (14) with $|S| = \pi r_0^2$ since

$(1/n)\Gamma(1/n) \rightarrow 1$. In case of a Gaussian envelope $n = 1$ or the Airy spot (8) with the same central mean intensity I_0 , one finds that the number of maxima above level u is smaller by a factor $(u/I_0)^{-1}$. This is, of course, expected, because a speckle pattern with a flat-top envelope presents a much larger surface area where the mean intensity is close to the maximal value I_0 .

C. The 2D focal volume

Most of the numerical simulations which study the growth of parametric instabilities in speckle patterns generated by RPP actually consider the following 2D case, which consists of one transversal dimension, say x , and one longitudinal dimension, say z . The field in the focal ‘‘line’’ is

$$A(x) = \frac{\sqrt{I_0}}{\sqrt{2N+1}} \sum_{j=-N}^N \exp i \left(\pi \frac{j}{N} \frac{x}{\rho_c} + \phi_j \right),$$

which implies that the field in the focal ‘‘volume’’ is given by

$$A(x,z) = \frac{\sqrt{I_0}}{\sqrt{2N+1}} \sum_{j=-N}^N \exp i \left(\pi \frac{j}{N} \frac{x}{\rho_c} - \frac{\pi^2}{4} \frac{j^2}{N^2} \frac{z}{z_c} + \phi_j \right).$$

In the asymptotic framework $N \gg 1$ the complex-valued field A obeys Gaussian statistics with mean 0 and correlation function:

$$C(x,z) = \frac{I_0}{2} \int_{-1}^1 ds \exp i \left(\pi s \frac{x}{\rho_c} - \frac{\pi^2}{4} s^2 \frac{z}{z_c} \right).$$

The real and imaginary parts of the field A obey the same Gaussian statistics with zero mean and the corresponding matrix of the second-order spectral moments is equal to

$$\Lambda = \frac{I_0}{2} \begin{pmatrix} \lambda_x & 0 \\ 0 & \lambda_z \end{pmatrix}, \tag{15}$$

where λ_ξ is defined by (13). Here we have $\lambda_x = \pi^2/(3\rho_c^2)$ and $\lambda_z = \pi^4/(80z_c^2)$. A very important fact is that the correlation function C has a nonzero imaginary part, which means that the real and imaginary parts of the field A are correlated. In particular the coefficient α defined by

$$i\alpha := \frac{\partial C}{\partial z}(0,0)/I_0 \tag{16}$$

is real and equal to $-\pi^2/(12z_c)$. This implies in particular that A_R and $\partial_z A_I$ are correlated in any point. As a consequence, close to a local maximum of the real part of the field, the partial derivative $\partial_z A_I$ is also very large which can be verified by applying Appendix A. We cannot apply the formulas of Sec. III to derive the statistics of local maxima of the field A , because the independence of the fields A_R and A_I was assumed in that section. In Appendix C we carefully study the 2D focal volume and come to the conclusion that there exists an effective matrix $\tilde{\Lambda}$ given by

$$\tilde{\Lambda} = \frac{I_0}{2} \begin{pmatrix} \lambda_x & 0 \\ 0 & (\lambda_z - \alpha^2) \end{pmatrix}, \tag{17}$$

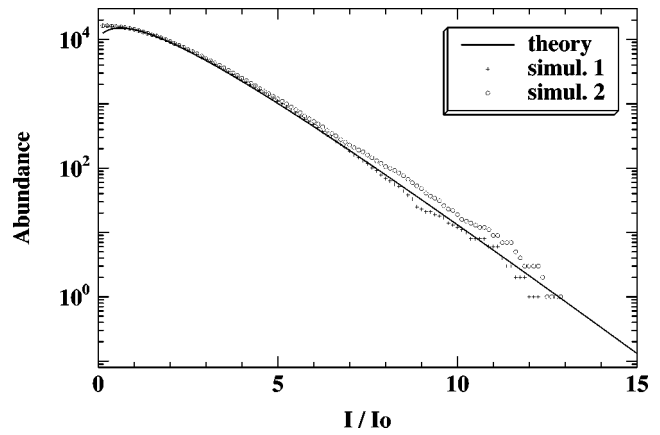


FIG. 5. Abundance M_I^{xz} of local maxima of the intensity above level I in a subdomain S of the 2D focal ‘‘volume.’’ Here $N=100$, $\rho_c=0.005$, $z_c=0.005$ and $|S|=2$. Results corresponding to two different simulations (crosses and circles) and the theoretical mean abundance (solid line) corresponding to Eq. (19) are shown.

which we must substitute for Λ in order to get the correct result:

$$\langle M_u^{xz} \rangle = \frac{4|S| |\det \tilde{\Lambda}|^{1/2}}{\pi^2 I_0} \left(\left(\frac{1}{2} + \frac{\pi}{4} \right) \frac{u}{I_0} + \frac{1}{2} \right) \exp - \frac{u}{I_0}, \tag{18}$$

where $|\det \tilde{\Lambda}|^{1/2} = I_0 \pi^3 / (12\sqrt{15}\rho_c z_c)$, and S is the reference surface. This formula is very similar to Eq. (5). The only but important difference comes from the fact that $\tilde{\Lambda}$ is not the matrix of the second-order spectral moments of the field A_R or A_I , but it is an effective matrix which captures all the relevant parameters of the statistical properties of the hot spots of the field. As explained in Appendix C, $\tilde{\Lambda}$ is the matrix corresponding to the field $\tilde{A}(x,z) := A(x,z) \times \exp(-iaz)$ whose hot spots obey the same statistics as those of A and whose correlation function has vanishing partial derivatives at 0. The above expression can then be simplified into

$$\langle M_u^{xz} \rangle = \frac{\pi|S|}{3\sqrt{15}\rho_c z_c} \left(\left(\frac{1}{2} + \frac{\pi}{4} \right) \frac{u}{I_0} + \frac{1}{2} \right) \exp - \frac{u}{I_0}, \tag{19}$$

which is plotted in Fig. 5.

D. The 3D focal volume

We now address the model of RPP developed in Sec. VI A. In some reference volume V where the mean intensity is almost constant and in the asymptotic framework $N \gg 1$ the complex-valued field A obeys Gaussian statistics with mean 0 and correlation function:

$$C(x,y,z) = \frac{I_0}{4} \int_{-1}^1 ds \int_{-1}^1 du \exp i \pi \frac{sx + uy}{\rho_c} \times \exp - i \frac{\pi^2 (s^2 + u^2) z}{4z_c}.$$

If $a = \lambda_0 f/h$ stands for the width of the overall envelope of the intensity distribution, then the diffraction length of the envelope is about $k_0 \rho_c a$. We therefore restrict ourselves to a

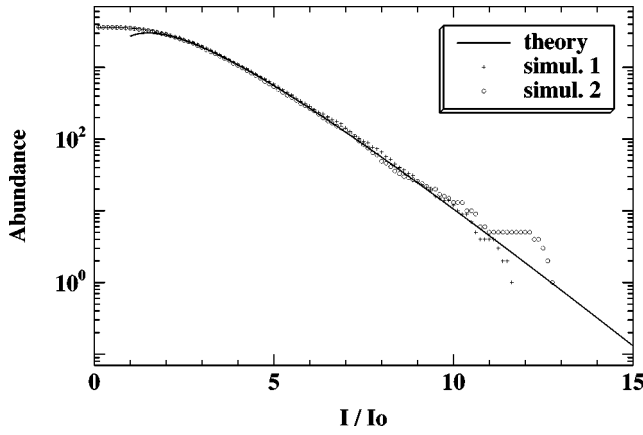


FIG. 6. Abundance M_l^{xyz} of local maxima of the intensity above level I in a subdomain V of the focal volume. Here $N=30$, $\rho_c=0.05$, $z_c=0.05$ and $|V|=2$. Results corresponding to two different simulations (crosses and circles) and the theoretical mean abundance (solid line) corresponding to Eq. (21) are shown.

reference volume V where the x, y -coordinates (resp. the z -coordinate) vary less than a (resp. $k_0 a \rho_c$). Adopting the notations (13)–(16) we have here $\lambda_x = \lambda_y = \pi^2 / (3\rho_c^2)$, $\lambda_z = (7\pi^4) / (180z_c^2)$ and $\alpha = -\pi^2 / (6z_c)$. As in the case of the 2D focal volume, the correlation function has a nonzero imaginary part. We then introduce the effective matrix $\tilde{\Lambda}$:

$$\tilde{\Lambda} = \frac{I_0}{2} \begin{pmatrix} \lambda_x & 0 & 0 \\ 0 & \lambda_y & 0 \\ 0 & 0 & (\lambda_z - \alpha^2) \end{pmatrix} \quad (20)$$

whose determinant has squared root equal to $|\det \tilde{\Lambda}|^{1/2} = I_0^{3/2} \pi^4 / (36\sqrt{5}\rho_c^2 z_c)$. Using exactly the same arguments as in Sec. VI C we find from Eq. (6) that the mean number of local maxima above the level u of the intensity $|A|^2$ is given by

$$\langle M_u^{xyz} \rangle = \frac{\pi^{3/2} \sqrt{5} |V|}{27\rho_c^2 z_c} \left(\left(\frac{u}{I_0} \right)^{3/2} - \frac{3}{10} \left(\frac{u}{I_0} \right)^{1/2} \right) \exp - \frac{u}{I_0}, \quad (21)$$

which is plotted in Fig. 6.

E. Discussion

Let us compare the results demonstrated in this paper with the ones which are derived in Refs. 10 and 11. First note that our proof is fully theoretical, and that there is no free parameter that we must fit in order to come to an agreement between simulations and theory. Second, we recall the formula obtained by Rose and DuBois:^{10,11}

$$\langle M_u^{xyz} \rangle |_{\text{R\&D}} = \frac{|V|}{\rho_c^2 z_c} A \left(\frac{u}{I_0} + B \right) \exp - \frac{u}{I_0}. \quad (22)$$

As shown by Fig. 7, the formula (21) is valid as soon as $u/I_0 > 2$, and remains valid for the whole range of values of the detected maximal intensities. In comparison formula (22) cannot fit the whole range of intensities and a clear bias is noticeable. Even in the case when one tries to fit the parameters as efficiently as possible, one will fall into the follow-

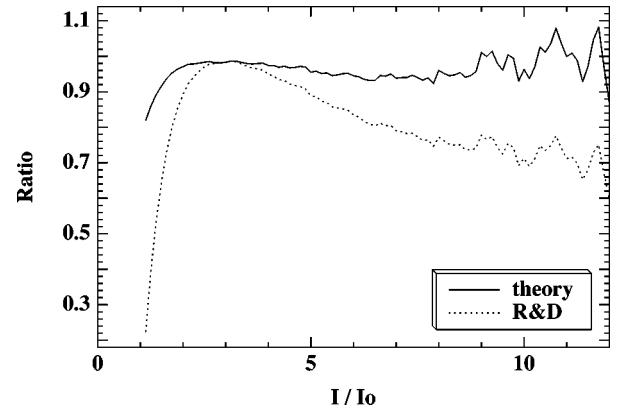


FIG. 7. Ratio of the theoretical abundance of local maxima above I over the simulated abundance for the corresponding configuration. The solid line stands for Eq. (21) and the dashed line for Rose and DuBois' formula (22) with the best fit $A=1.2$ and $B=-1.0$. Here $N=50$, $\rho_c=0.025$, $z_c=0.025$ and $|V|=1.5$. The dashed curve is below the ideal line "ratio=1," which means that the formula (22) finds less hot spots than there exist actually.

ing trap. Indeed one has to fit the parameters by using numerical simulations in the area $u/I_0 \in [3, 6]$. But then one will observe an important departure in the area $u/I_0 \in [10, 15]$ which corresponds to the very intense hot spots which are very relevant in the point of view of parametric instabilities growth. This departure is in the sense of an underestimate of the number of very intense spots which is of order of 30% in the configuration of Fig. 7.

To be complete we add the following comment. The results presented in Secs. VI B–VI D hold true for a square RPP, which corresponds to a square near-field beam. Indeed this configuration will be implemented in the LMJ and the NIF. Nevertheless, many other laser facilities produce circular near-field beams, so it is convenient to reformulate the above results in case of a circular RPP and near-field beam with radius $D/2$. This is equivalent to a top hat model for the RPP energy spectrum which is uniform for perpendicular wave numbers $\mathbf{k}=(k_x, k_y)$ such that $|\mathbf{k}| \leq k_0 / (2F)$ (where $F=f/D$), and vanishes outside this disk. Then, defining ρ_c and z_c as (10) and (11), the mean numbers of local maxima above the level u in some surface S inside the focal plane and in some volume V inside the focal volume read respectively as

$$\langle M_u^{\text{circ-xy}} \rangle = \frac{|S|}{\rho_c^2} \left(\left(\frac{1}{2} + \frac{\pi}{4} \right) \frac{u}{I_0} + \frac{1}{2} \right) \exp - \frac{u}{I_0},$$

$$\langle M_u^{\text{circ-xyz}} \rangle = \frac{5\pi^{3/2} |V|}{48\sqrt{6}\rho_c^2 z_c} \left(\left(\frac{u}{I_0} \right)^{3/2} - \frac{3}{10} \left(\frac{u}{I_0} \right)^{1/2} \right) \exp - \frac{u}{I_0}.$$

VII. APPLICATION TO THE SPECKLE PATTERN GENERATED BY A KPP

We finally discuss the extensions of the results of Sec. VI to the KPP configuration. There are many ways to design a KPP. The usual method¹⁴ consists in carefully and adiabati-

cally modifying an initial random phase screen so as to get a speckled far-field that has a flat top super Gaussian envelope. Since the induced focal spot results from the superposition of many independent modes the central limit theorem can still be applied, which implies that the statistics of the far field is Gaussian. This statement is confirmed by recent numerical simulations which show that the histogram of the intensity is exponential, which is characteristic of a standard speckle pattern. Unfortunately, it is not so obvious to theoretically compute the correlation function of the far field. For this purpose let us regard the optical transfer function which is proportional to the Fourier transform of the far-field intensity (Ref. 21, Section 8.1):

$$\mathcal{H}(v_x, v_y) = \frac{1}{|S_{kpp}|} \int_{S_{kpp}} \mathbb{1}_{(x-\lambda_0 f v_x, y-\lambda_0 f v_y) \in S_{kpp}} \exp i(\phi(x, y) - \phi(x - \lambda_0 f v_x, y - \lambda_0 f v_y)) dx dy,$$

where S_{kpp} is the surface of the KPP. If we assume that the spatial statistics of the phase screen are wide-sense stationary and ergodic, then the optical transfer function of the far field factors into the product:

$$\mathcal{H}(v_x, v_y) = \mathcal{H}_0(v_x, v_y) \mathcal{H}_s(v_x, v_y),$$

where \mathcal{H}_0 is the optical transfer function of the phase plate without the phase modulation:

$$\mathcal{H}_0(v_x, v_y) = \frac{1}{|S_{kpp}|} \int_{S_{kpp}} \mathbb{1}_{(x-\lambda_0 f v_x, y-\lambda_0 f v_y) \in S_{kpp}} dx dy,$$

and \mathcal{H}_s is the normalized spatial autocorrelation function of the transmittance of the phase plate:

$$\mathcal{H}_s(v_x, v_y) = \Gamma_t(\lambda_0 f v_x, \lambda_0 f v_y),$$

$$\Gamma_t(\Delta x, \Delta y) = \mathbb{E}[\exp i(\phi(x, y) - \phi(x + \Delta x, y + \Delta y))].$$

The characteristic scales of \mathcal{H}_0 and \mathcal{H}_s are very different, so that \mathcal{H}_0 will impose the small-scale variations of the far field, while \mathcal{H}_s will impose the shape of the overall envelope. More exactly, if the near field is square, then we have

$$\mathcal{H}_0(v_x, v_y) = \Lambda(v_x \rho_c) \Lambda(v_y \rho_c),$$

where $\Lambda(\alpha) = 1 - |\alpha|$ if $|\alpha| \leq 1$ and 0 otherwise, and $\rho_c = \lambda_0 f / D$ is consequently the correlation radius of the fine-scale fluctuations of the focal spot. Furthermore, in case of a binary RPP, we have $\Gamma_t(\Delta x, \Delta y) = \Lambda(\Delta x / h) \Lambda(\Delta y / h)$ where h is the size of a square element of the RPP, so that the envelope of the focal spot is an Airy function with width $\lambda_0 f / h$. In the case of a smooth phase screen with Gaussian statistics, the envelope of the focal spot has Gaussian shape (Ref. 21, Section 8.3). In the case of a KPP, the statistical stationarity condition of the phase screen may be not strictly fulfilled, since small modifications are imposed to an initial random phase screen so as to modify the envelope of the far field and to get a super-Gaussian envelope. Nevertheless, one can expect that the factorization still holds true qualitatively in the sense that the fine-scale statistics of the far field is essentially imposed by the global shape of the near-field beam, while the overall envelope of the far-field is determined by the variations of the fine-scale phase screen.

Within this framework, the matrices of the second-order spectral moments are similar for a square (resp. circular) RPP and for a square (resp. circular) KPP, and one can apply directly the results of Sec. VI. Nevertheless, we feel that it should be relevant to include in the computer algorithms that design the phase screens the task which consists in estimating precisely the form and width of the correlation function of the far-field pattern generated by the KPP. With such information one can compute with accuracy the matrix Λ as (12) and (13) and then apply (5) to obtain the expected number of hot spots above level u in the total focal spot S . Similarly one can compute the matrix $\tilde{\Lambda}$ as (20), (13), and (16) and then apply (6) to obtain the expected number of hot spots above level u in the total focal volume V .

VIII. CONCLUSION

The control of high intensities of smoothed beams is a difficult but crucial problem for ICF applications so as to limit the growth of plasma instabilities which may be responsible for energetic losses. The shape of the focal spot can be optimized by using a KPP,¹⁴ so that the averaged intensity is limited to a value below 10^{15} W/cm². Nevertheless this value is still too close to the instability threshold, because the high fluctuations of the resulting partially coherent beam makes some hot spots exceed this critical value. Under such conditions, several authors who consider either stimulated Brillouin scattering (SBS),¹¹ or both self-focusing and SBS,^{7,9} have pointed out that the reflectivity from plasma will be proportional to the number $M_{u_c}^{xyz}$ of speckles in the focal volume that will be over some critical value u_c . This argument holds true whenever $u_c \gg I_0$, so that the underlying hypothesis of independence of the hot spots above u_c can be considered as reasonable. This regime is precisely the regime which is expected for the future megajoule-scale lasers. We have just demonstrated that the statistical theory of hot spots which has been used in the last decade underestimates the number of the most intense hot spots. We feel that this could give rise to noticeable departures when substituting a more accurate estimate of $\langle M_{u_c}^{xyz} \rangle$ into the already existing formulas for the average reflectivity by a macroscopic plasma.

Let us end this paper with a final remark. One can observe in all numerical simulations that the global maximum, or even the two or three most intense spots of the whole pattern, do not present a deterministic behavior, but exhibit rather important fluctuations. It should then be of great interest to find a precise description of the statistical properties of this global maximum. Indeed it will be a relevant estimate of the SBS threshold, defined as a condition where at least one hot spot appears in the active area $M_{u_c}^{xyz} \geq 1$. This work is in progress and will be the subject of a further paper.

ACKNOWLEDGMENTS

The author thanks S. Hüller for useful and stimulating discussions. This research was performed under the auspices of the Laser MegaJoule program of Commissariat à l'Énergie Atomique.

APPENDIX A: A FUNDAMENTAL LEMMA OF PROBABILITY

Let us consider a \mathbb{R}^2 -valued Gaussian vector (X, Y) with mean $(0, 0)$ and covariance:

$$\begin{pmatrix} \langle X^2 \rangle & \langle XY \rangle \\ \langle XY \rangle & \langle Y^2 \rangle \end{pmatrix} = \begin{pmatrix} \sigma_X^2 & \alpha \\ \alpha & \sigma_Y^2 \end{pmatrix}.$$

Then, conditionally to $X=x$, the real-valued variable Y obeys Gaussian statistics with mean $\alpha x/\sigma_X^2$ and variance $\sigma_Y^2 - \alpha^2/\sigma_X^2$.

APPENDIX B: ANSATZ

In this appendix we check the accuracy of the ansatz applied in Sec. III. Let us consider that at $\mathbf{x}=0$ lies a local maximum of A_R^2 and denote $a_R^2 := A_R^2(0)$. Applying Appendix A with $(A_R(0), \partial_{x_j}^2 A_R(0))$, and taking into account the fact that $\partial_{x_j} A_R(0) = 0$, we have in the neighborhood of 0

$$A_R(\mathbf{x}) = a_R \left(1 - \frac{1}{2} \sum_{j=1}^d \lambda_j x_j^2 \right) + \dots, \tag{B1}$$

$$A_I(\mathbf{x}) = A_I(0) + \sum_{j=1}^d \frac{\partial A_I}{\partial x_j}(0) x_j + \dots, \tag{B2}$$

where $A_I(0)$ and $\partial_{x_j} A_I(0), j=1, \dots, d$, are independent from each other and independent from $A_R(0)$. $A_I(0)$ obeys Gaussian statistics with mean 0 and variance $I_0/2$, and $\partial_{x_j} A_I(0)$ obeys Gaussian statistics with mean 0 and variance $\lambda_j I_0/2$. As a consequence the maximum of $|A|^2 = A_R^2 + A_I^2$ is not reached in 0, but in \mathbf{x}_m whose coordinates are

$$x_j = \frac{A_I(0) \partial_{x_j} A_I(0)}{\lambda_j a_R^2} + O\left(\left(\frac{I_0}{a_R^2}\right)^2\right), \quad j=1, \dots, d.$$

Note that $\sqrt{\lambda_j} x_j = O(I_0/a_R^2)$ which is small in the case of a large maximum a_R^2 . This justifies the fact that we have only taken into account the first terms in the expansions (B1) and (B2). Therefore the corresponding maximum is

$$|A|^2(\mathbf{x}_m) = a_R^2 + A_I^2(0) + \frac{A_I^2(0)}{a_R^2} Z_d, \tag{B3}$$

$$Z_d := \sum_{j=1}^d \frac{(\partial_{x_j} A_I(0))^2}{\lambda_j}. \tag{B4}$$

Here Z_d obeys a gamma distribution with mean $dI_0/2$ and density $p_d(z) = 1/(\Gamma((d+1)/2) I_0) (z/I_0)^{(d-1)/2} e^{-z/I_0}$. The first term in the right-hand side of (B3) is the dominant one, the second term is a first order correction, while the last term in the sum is of second order and brings a contribution which will be neglected. This completes the demonstration of the ansatz.

APPENDIX C: THE 2D FOCAL VOLUME

In this appendix we study carefully the configuration presented in Sec. VI C. Let us assume that at $\mathbf{x}=0$ lies a local maximum of A_R^2 . Applying Appendix A with

$(A_R(0), \partial_z A_I(0))$ and $(\partial_z A_R(0), A_I(0))$, we get that, given $A_R(0) = a_R$ and $\partial_z A_R(0) = 0$, we have

$$A_I(0) \sim \mathcal{N}\left(0, \frac{I_0}{2} \left(1 - \frac{\alpha^2}{\lambda_z}\right)\right), \tag{C1}$$

$$\frac{\partial A_I}{\partial z}(0) \sim \mathcal{N}\left(\alpha a_R, \frac{I_0}{2} (\lambda_z - \alpha^2)\right). \tag{C2}$$

Here and in the following $X \sim \mathcal{N}(a, \sigma^2)$ is a shorthand for ‘‘ X obeys Gaussian statistics with mean a and variance σ^2 .’’ More generally every odd-order partial derivatives of A_I with respect to z are affected in that they obey Gaussian statistics with means proportional to a_R , while every even-order partial derivatives of A_I with respect to z are affected in that they obey Gaussian statistics with reduced variances. It is obvious that at least the fact that $\partial_z A_I(0)$ is very large will produce a departure from the formulas obtained in Sec. III and Appendix B. Nevertheless we can efficiently bypass the problem by using the following trick. We consider the field \tilde{A} which is simply the field A changed by a deterministic phase factor:

$$\tilde{A}(x, z) = A(x, z) \exp -i\alpha z.$$

We also denote by \tilde{A}_R and \tilde{A}_I the real and imaginary parts of \tilde{A} , and by \tilde{C} the correlation function of the field \tilde{A} . The statistics of the hot spots of A and \tilde{A} are obviously identical. Furthermore, we have

$$\frac{\partial \tilde{C}}{\partial z}(0, 0) = 0,$$

and consequently the correlations between the field and its first-order spatial derivatives are canceled. Given $\tilde{A}_R(0) = a_r$ and $\partial_\zeta \tilde{A}_R = 0$ for $\zeta = x, z$, the imaginary part of the field and its first partial derivatives then obey the zero-mean distributions:

$$\tilde{A}_I(0) \sim \mathcal{N}\left(0, \frac{I_0}{2}\right), \tag{C3}$$

$$\frac{\partial \tilde{A}_I}{\partial x}(0) \sim \mathcal{N}\left(0, \frac{I_0}{2} \lambda_x\right), \tag{C4}$$

$$\frac{\partial \tilde{A}_I}{\partial z}(0) \sim \mathcal{N}\left(0, \frac{I_0}{2} (\lambda_z - \alpha^2)\right), \tag{C5}$$

but the second derivative with respect to z of \tilde{A}_R obeys

$$\frac{\partial^2 \tilde{A}_R}{\partial z^2} \sim \mathcal{N}\left((\alpha^2 - \lambda_z) a_R, \frac{1}{2} \left| \frac{\partial^4 \tilde{C}}{\partial z^4} - \frac{1}{2I_0} \left| \frac{\partial^2 \tilde{C}}{\partial z^2} \right|^2 \right.\right).$$

In fact, this is connected with the fact that the matrix $\tilde{\Lambda}$ of the second-order spectral moments of the real-valued Gaussian process \tilde{A}_R is given by (17), whose expression is different from Λ . As a consequence, if we assume that 0 is a local maximum of \tilde{A}_R^2 at level a_R^2 , then in the neighborhood of 0 the real and imaginary parts of \tilde{A} are given by

$$\tilde{A}_R(\mathbf{x}) = a_R \left(1 - \frac{1}{2} \lambda_x x^2 - \frac{1}{2} (\lambda_z - \alpha^2) z^2 \right) + \dots, \tag{C6}$$

$$\tilde{A}_I(\mathbf{x}) = \tilde{A}_I(0) + \frac{\partial \tilde{A}_I}{\partial x}(0)x + \frac{\partial \tilde{A}_I}{\partial z}(0)z + \dots, \quad (\text{C7})$$

where $\tilde{A}_I(0)$ and $\partial_z \tilde{A}_I(0)$ obey the distributions (C3)–(C5). We then reproduce the same arguments as in Sec. III and Appendix B [substitute Eqs. (C6) and (C7) for Eqs. (B1) and (B2)], we check that the higher-order terms in the expansions (C6) and (C7) give rise to negligible contributions to the statistics of hot spots, and we finally establish (18).

¹M. André, in *Technical Committee Meeting on Drivers and Ignition facilities for Inertial Fusion*, edited by J. Coutant, Proceedings of the International Atomic Energy Agency (CEA/DAM Publications, Limeil-Valenton, France, 1995).

²R. W. Short, W. Seka, and R. Bahr, *Phys. Fluids* **30**, 3245 (1987).

³A. N. Mostovych, S. P. Obenschain, J. H. Gardner, J. Grun, K. J. Kearney, C. K. Manka, E. A. McLean, and C. J. Pawley, *Phys. Rev. Lett.* **59**, 1193 (1987).

⁴S. Baton, C. Labaune, G. Mathieussant, and W. Seka, *Opt. Commun.* **70**, 50 (1989).

⁵O. Willi, T. Afshar-rad, S. Coe, and A. Giulietti, *Phys. Fluids B* **2**, 1318 (1990).

⁶C. Labaune, S. Baton, T. Jalinaud, H. Baldis, and D. Pesme, *Phys. Fluids B* **4**, 2224 (1992).

⁷H. A. Rose, *Phys. Plasmas* **2**, 2216 (1995).

⁸V. T. Tikhonchuk, P. Mounaix, and D. Pesme, *Phys. Plasmas* **4**, 2670 (1997).

⁹V. T. Tikhonchuk, S. Hüller, and P. Mounaix, *Phys. Plasmas* **4**, 4369 (1997).

¹⁰H. A. Rose and D. F. DuBois, *Phys. Fluids B* **5**, 590 (1993).

¹¹H. A. Rose and D. F. DuBois, *Phys. Rev. Lett.* **72**, 2883 (1994).

¹²J. Garnier, C. Gouédard, L. Videau, and A. Migus, *J. Opt. Soc. Am. A* **14**, 1928 (1997).

¹³Y. Kato, K. Mima, N. Miyanaga, S. Arinaga, Y. Kitagawa, M. Nakatsuka, and C. Yamanaka, *Phys. Rev. Lett.* **53**, 1057 (1984).

¹⁴S. N. Dixit, M. D. Feit, M. D. Perry, and H. T. Powell, *Opt. Lett.* **21**, 1715 (1996).

¹⁵J. Adler, *The Geometry of Random Fields* (Wiley, New York, 1981).

¹⁶C. Delmas, *C. R. Acad. Sci. Paris I* **327**, 393 (1998).

¹⁷D. Middleton, *Introduction to Statistical Communication Theory* (McGraw-Hill, New York, 1960).

¹⁸S. Pau, S. N. Dixit, and D. Eimerl, *J. Opt. Soc. Am. B* **11**, 1498 (1994).

¹⁹S. N. Dixit, I. M. Thomas, B. W. Woods, A. J. Morgan, M. A. Hennesian, P. J. Wegner, and H. T. Powell, *Appl. Opt.* **32**, 2543 (1993).

²⁰J. W. Goodman, in *Laser Speckle and Related Phenomena*, edited by J. C. Dainty, Topics in Applied Physics, Vol. 9 (Springer-Verlag, Berlin, 1984), pp. 9–75.

²¹J. W. Goodman, *Statistical Optics* (Wiley, New York, 1985).